ANALYZING POWER MEASUREMENTS AND THE NUCLEON-NUCLEUS OPTICAL POTENTIAL; A FOCUS ON THE SPIN-ORBIT POTENTIAL

Richard L. Walter
Department of Physics
Duke University and Triangle Universities Nuclear Laboratory
Durham, North Carolina 27708-0308

Abstract

The spin-orbit interaction obtained in optical model (OM) searches on nucleon-nucleus scattering is reviewed. Although some single-energy OM search results are given, the main focus is on global OMs that incorporated a reasonable amount of polarization data. A corrected table of the Walter-Guss (WG) OM parameters is included. An outline of neutron $A_y(\theta)$ experimental method of the TUNL group is presented, along with an overview of TUNL projects for interpreting the $A_y(\theta)$ data: i) the WG optical model, ii) the dispersive optical model, and iii) the microscopic model.

I. Introduction

The present paper will stress three topics related to the optical model for nucleon-nucleus scattering for energies above 10 MeV. First, a review of global optical models for neutron and proton scattering in the 10 to 180 MeV region, with an emphasis on polarization data and the nature of the spin-orbit interactions presented. Second an overview of neutron polarization measurements conducted at the Triangle Universities Nuclear Laboratory (TUNL) and a presentation of sample proton polarization data is given. Third, a discussion of several of the approaches used at TUNL to interpret the neutron polarization data is reported. Because the length of the present paper is restricted, the descriptions on all of the topics necessarily will be brief and incomplete; we do not pretend to present all the important work on polarization measurements or optical models here. An introduction to the optical model (OM) concept and a fairly comprehensive review of OM work prior to 1971 is given in Hodgson's textbook [1]; a compilation of OM parameters for the early 1970s is given in the report by the Pereys [2]. A concise summary of the isovector terms of the OM potential connecting neutron scattering to proton scattering and (p,n) reactions is presented in Rapaport's OM review [3].

Measurements of the analyzing power $A_y(\theta)$ for nucleon scattering from nuclei have provided sensitive information about the nature of the nucleon-nucleus spin-orbit interaction. This interaction potential is known to have a real and an imaginary part. Below 60 MeV the imaginary part is small and has a negligible effect on the differential cross section $\sigma(\theta)$. However, the real part has an important influence on the $\sigma(\theta)$ in this energy range, as evidenced by large analyzing powers for neutron scattering above a few MeV and for proton scattering at energies where Coulomb scattering does not dominate, i.e., for $E > 7$ MeV for medium-weight nuclei and for $E > 20$ MeV for heavy nuclei.

The present paper presents a sample of neutron-nucleus polarization data for neutron energies $5 \leq E_n \leq 17$ MeV and for proton energies $16 \leq E_p \leq 180$ MeV. The measurements of our group, which fall into the former category, are more difficult to perform than proton measurements since: i) there are no direct sources of polarized neutron beams in contrast to the case for proton beams obtained with atomic-beam polarized ion sources; ii) compared to proton detectors, which have 100% efficiency, neutron detectors used in polarization studies typically have less than 30% efficiency; iii) neutron spectrometry is very inefficient, normally requiring pulsed-beam time-of-flight methods. This accounts for the scarceness of neutron polarization data and the large statistical uncertainties for neutron data compared to proton data. A very brief description about the neutron time-of -flight method at TUNL will be presented.

II. Review of global optical models and spin-orbit term

Early phenomenological optical models for neutrons, like the one Wilmore and Hodgson [4] provided in 1964, ignored the spin-orbit interaction because the emphasis was to provide a model that described (and predicted) the main features of neutron scattering cross sections. In fact, there were insufficient neutron polarization data to constrain the magnitude and the energy dependence of the spin-orbit interaction at this time. In 1963 Perey [5] produced an OM for $27 \leq A \leq 197$ for $9 \leq E_p \leq 22$ MeV which incorporated some polarization data and which provided much understanding and groundwork for global optical models. Perhaps the most classic work [6] is that reported in 1969 by Becchetti and Greenlees (BG) for $A > 40$ for $7 \leq E_p \leq 40$ MeV and for $1 \leq E_n \leq 24$ MeV. It provided the parameters for many reaction calculations since its publication. Although today their OM is known to be an inaccurate predictor for neutron scattering $\sigma(\theta)$ and $A_y(\theta)$ distributions within its expected range of applicability, it is still often used for neutrons because of its simplicity and its acceptance over the past three decades for proton-induced reactions. The determination of the spin-orbit interaction by BG was based solely on proton analyzing power measurements. In 1979 Rapaport, Kulkarni and Finlay [7] reported a neutron-nucleus model for $40 \leq A \leq 208$ based on $\sigma(\theta)$ data from 7 to 26 MeV and adopted the BG spin-orbit interaction because no polarization data were included.

Shortly after the BG report appeared, Menet et al. [8] from ORNL published a proton OM for $30 \leq E_p \leq 60$ MeV that heavily weighted their own total reaction cross sections and on ORNL $\sigma(\theta)$ and $A_y(q)$ data. They used the spin-orbit parameters taken from an earlier analysis of the $\sigma(\theta)$and $A_y(\theta)$ by two of the same authors.[9] In 1982 Schwandt et al. [10] measured $A_y(\theta)$ for protons at a few energies in the energy range between 60 and 180 MeV for seven nuclei in the range $24 \leq A \leq 208$. Combining these data with their $\sigma(\theta)$ data, Schwandt et al. conducted an OM search to obtain a model for protons over this energy range. It is noteworthy that by 180 MeV the depth of the real central potential has dropped to about 18 MeV (from about 50 MeV at E_p=0) and the strength of the real spin-orbit has dropped to about 2.5 MeV (from about 6 MeV at E_p=0 MeV), but the magnitude of the imaginary spin-orbit strength has increased to about 2 MeV. Thus, at 180 MeV (and higher) the spin-orbit interaction has a large influence on the scattering process, e.g., the cross section. The $A_y(\theta)$ has changed from a function that strongly oscillates through a value of 0.0 to a function that has small oscillations between values in the localized region from +0.8 and +1.00. In fact, the data of [10] was key to recognizing the need for incorporating the imaginary part $W_{so}(E)$ of the spin-orbit interaction. This term usually had been neglected in OM potentials prior to their work.

Two more recent “global” optical models that focused heavily on polarization data deserve mention here. In 1985 Walter and Guss (11) developed a neutron OM for $E_n \geq 10$ MeV using $\sigma(\theta)$ and total cross-section data σ_T plus a wealth of $A_y(\theta)$ data from measurements at TUNL. The mass range was restricted to $A \geq 54$ in order to avoid the complications associated with A-dependent quantities required in global models when lighter mass nuclei are included. The lower limit of 10 MeV was selected in order to be free from significant compound-nucleus formation and complicated energy dependences of the strength and radius of the real central term between $0 \leq E_n \leq 10$ MeV, a problem that was later explained as a result of the dispersion term (discussed below). Most of the $\sigma(\theta)$ data employed by WG was for $10 \leq E_n \leq 26$ MeV, but the (limited amount of) data [12] available at 30 and 40 MeV were included in the data base for the global search. Walter and Guss

constrained the energy dependence of some of the terms so that they would approximately connect onto those of Schwandt et al. This constraint included consideration of the isovector terms for the real central and real spin-orbit interaction. They also forced the energy dependence of the real and imaginary spin-orbit terms to be similar to that of Schwandt et al. In retrospect, these constraints have proven to be important for being able to use the WG model up to 80 MeV. To test the reasonableness of the isovector terms, WG included the Coulomb potential and calculated $\sigma(\theta)$ and $A_y(\theta)$ for a few nuclei between 16 and 80 MeV proton scattering; the predictions were quite favorable (see Figure 4 of WG), suggesting that the model might be very suitable for proton energies extending out to the 80 MeV where the Schwandt et al. model is designed to start.

The last global OM for heavy nuclei to be discussed here is the one obtained by Varner et al. [13] in 1991 from the analysis of proton $\sigma(\theta)$ and $A_y(\theta)$ data from 16 to 65 MeV and neutron $\sigma(\theta)$ and $A_y(\theta)$ from 10 to 26 MeV for nuclei with $40 \leq A \leq 209$. These authors were guided in the design of the dependences on A by microscopic model considerations. They introduced A-dependences into the radius parameters that were in addition to the usual $R = r_0A^{1/3}$; this modification impacts the strength of the isovector terms and complicates comparisons to Schwandt et al., for example. Although the energy range was fairly large, they could not establish the need for an energy dependence for the real spin-orbit term. Furthermore, as the predominant modeling was performed with proton data, they did not recognize the need for an imaginary spin-orbit ($W_{so}(E)$) term, much less its energy dependence. This latter difficulty is not too surprising as we know that $W_{so}(E)$ is small in magnitude below 65 MeV and passes through zero somewhere in the region near 50 to 60 MeV. However, by ignoring the data and energies of Schwandt et al., Varner et al. conclude that the V_{so} is constant with E_p, and subsequently, with E_n. It is risky to extend their constant V_{so} into the region $E_p \geq 100$ MeV where the strength of the real central potential is of the order of their V_{so}, i.e., where scattering and reaction predictions will be highly dependent on the parametrization of $V_{so}(E)$ and $W_{so}(E)$.

The group of Sakaguchi et al. [14] performed the high-accuracy proton measurements of $\sigma(\theta)$ and $A_y(\theta)$ at 65 MeV that were later employed in the model of Varner et al. Sakaguchi et al. also made a careful OM analyses of these data, but concentrated only on their 65 MeV data. The measurements were for four nuclei for $40 \leq A \leq 208$. They did not attempt to formulate the A-dependences exhibited in their tabulated OM parameters, e.g., in their nuclear radius parameters, the difusenesses, and the potential strengths. They were able to fit the data without a $W_{so}(E)$ term. However, in a follow-up measurement Sakaguchi et al. [15] measured the (polarization) rotation parameter $R(\theta)$ at 65 MeV for four nuclei with $40 \leq A \leq 208$. In this analysis they found that it was necessary to include a $W_{so}(E)$ term with strengths ranging from -200 to -600 keV in order to fit $\sigma(\theta)$, $A_y(\theta)$ and $R(\theta)$. (Some of their data and calculations will be shown later.) This range of W_{so} values is consistent with those of Schwandt et al. and WG.

For light nuclei Watson, Singh and Segel [16] developed a global model for nine isotopes with $6 \leq A \leq 16$ for $10 \leq E_p \leq 50$ MeV. The focus of the present paper is for $A > 40$, so this work will not be discussed here other than to say that they suggested to replace with a constant the 1/r factor in the Thomas form factor of the spin-orbit interaction in order to keep the interaction from taking on abnormally large values as r approaches zero. They did introduce an isovector dependence term similar to that of Perey [5], which allowed them to predict neutron scattering. In their judgment, their OM "can give a good description of the general features of nucleon scattering from light nuclei", but a more thorough search using present day computers should lead to a better model.

III. Neutron Ay(θ) measurements at TUNL

The measurement of $A_y(\theta)$ involves measuring the scattering cross section at a fixed angle when the incident neutron beam is polarized along the normal to the scattering plane and comparing it to the cross section when the beam is polarized in the opposite direction. This method of using alternate orientations of the polarization direction eliminates the need to know the detector efficiency. To double the total number of counts and to cancel some intrinsic instrumental asymmetries, one uses a second detector located at the same angle but

on the opposite side of the incoming beam axis. The arrangement at TUNL for $A_y(\theta)$ measurements is shown in Figure 1 with three detedtor pairs. An incident beam of pulsed and polarized deuterons are accelerated in an FN tandem Van de Graaff and are incident on a deuterium gas cell. Neutrons emitted at $\theta = 0°$ from the $^2H(d,n)^3He$ reaction are polarized at a level of approximately 90% of the vector polarization of the deuteron beam, which is typically 60% to 70% at TUNL. These neutrons are scattered from cylindrical samples located about 10 cm from the deuterium cell. With the available deuteron energies at TUNL (1 to 17 MeV), this reaction provides polarized neutrons from 4 to 20 MeV. The overall time resolution of the detected neutrons is about 2 ns and the maximum flight paths are 6 m (left side) and 4 m (right side). This combination limits the nuclei for which we can resolve the elastically scattered neutrons from inelastically scattered to light nuclei and to nuclei around closed shells. We have investigated the $A_y(\theta)$ for about 20 nuclei in the energy range from 8 to 17 MeV for $18° \leq \theta \leq 155°$. For a few nuclei we have data up to 19 MeV and down to 5 MeV. A sample of the data is shown in Figure 2 alongside some OM calculations discussed later. Other than a set of data obtained for six nuclei at 8 MeV in Stuttgart by Hammer's group [17], the TUNL data are the only high accuracy $A_y(\theta)$ data in the 5 to 20 MeV region. There does exist neutron $A_y(\theta)$ data out to 75° at for six nuclei [18] 24 MeV and from 13° to 38° and 57° to 84° from the Alberta group [19] for ^{16}O, ^{59}Co and Pb at 23 MeV.

Figure 1. Arrangement at TUNL for $A_y(\theta)$ measurements for neutrons using the pulsed-beam time-of-flight method with detectors on the left and right sides to reduce instrumental asymmetries

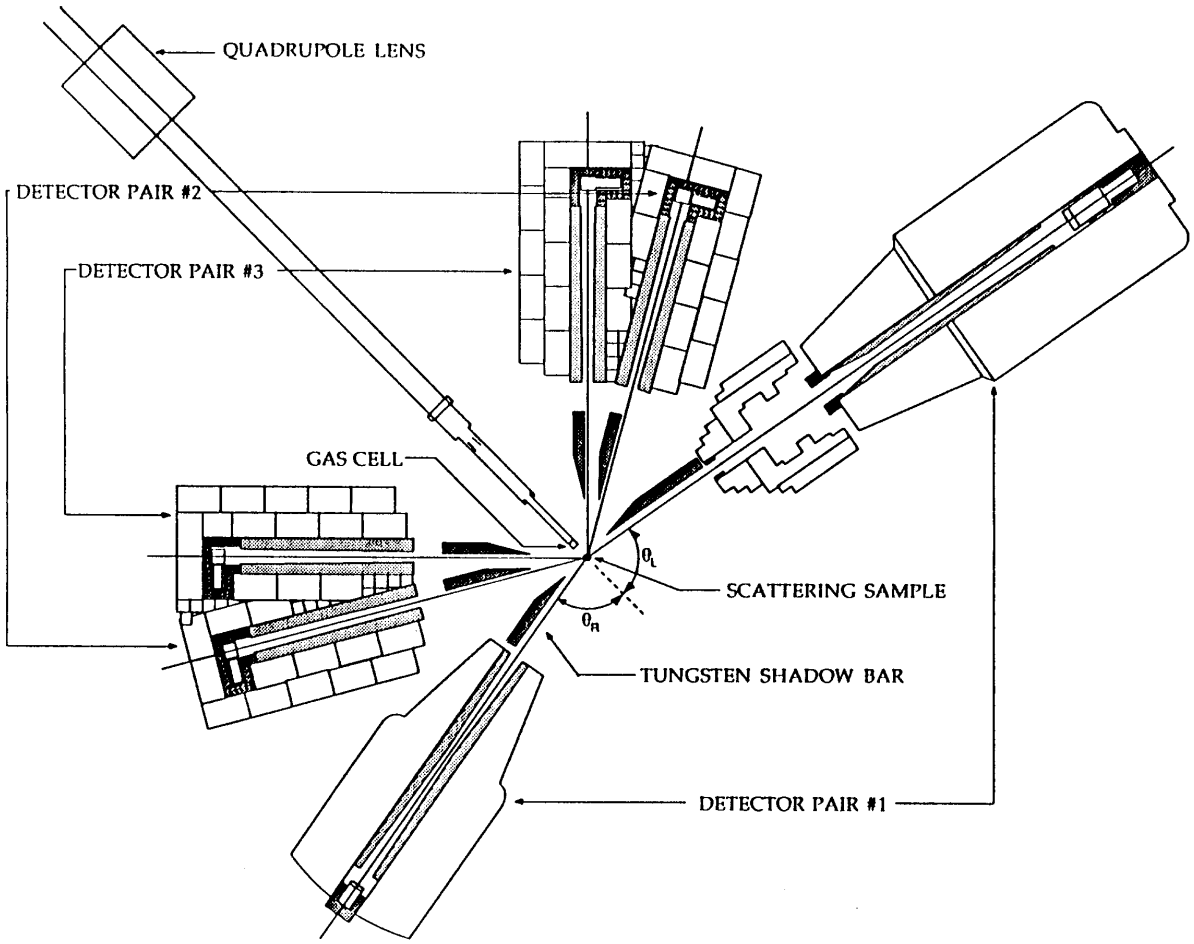

Figure 2. Typical TUNL data for $A_y(\theta)$; the curves are calculations [22] discussed near the end of Section IV

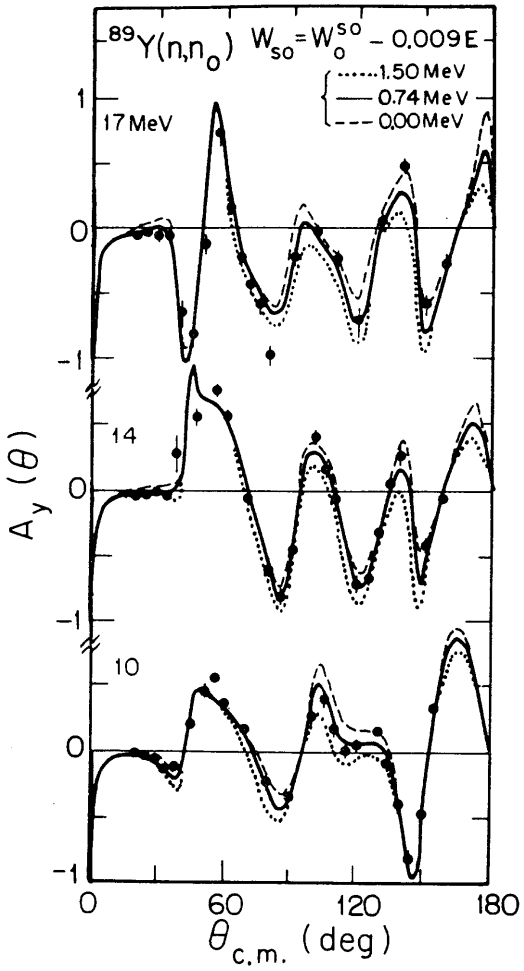

IV. TUNL OM analyses 1: Global analyses

Three "global" OM analyses have been performed at TUNL. One was an analysis of neutron and proton elastic-scattering $\sigma(\theta)$ for p-shell nuclei by Dave and Gould (DG) [20] in 1983. The energy range was from 7 to 15 MeV and much of the data for neutrons was measured at TUNL. No polarization data was included in this analysis. DG used the spin-orbit strength and radius of Watson et al. [16] and a slightly larger diffuseness. Because their analysis did not include polarization data, their spin-orbit parameters are not included in the table below.

Another TUNL product is the global OM referred to above as the work of Varner et al. The 16-MeV proton $\sigma(\theta)$ and $A_y(\theta)$ data used in their analysis was measured at TUNL by Varner's group and much of the neutron $\sigma(\theta)$ and $A_y(\theta)$ data was obtained at TUNL by our group. One criticism of the neutron analysis is that Varner et al. did not include total cross-section data in the search nor in the comparisons to calculations.

The other global model is the one discussed above that was developed by Walter and Guss specifically for neutrons in the energy range $10 \leq E_n \leq 40$ MeV, but one that appears to give reasonable predictions up to 80 MeV. This work was reported in the proceedings of an international conference on nuclear data. However, a problem arose when the publishers were changed during the publication process and the final manuscript was

lost. Unfortunately, an earlier version of the manuscript that contained some typographical errors and omissions was substituted by the publishers and printed. Because this potential is frequently used in calculations for nuclear applications and some users might not have been alerted to this publishing problem, we tabulate the correct parametrization here. However, first we write the normal OM formulae to define the symbols. The general formulae introduced here are the same as those used in all the OMs mentioned in Section II, even to the extent that they all used the same radial forms of the potentials, i.e., Woods-Saxon (WS) for volume terms (real and absorption) and derivative Woods-Saxon for the surface terms (absorption and spin-orbit).

The optical-model potential is written as:

$$\begin{aligned} U(r,E) = &-\{V_V + iW_V\} f_V(r,R_V,a_V) + V_C(r) \\ &+ i\{4a_S W_S\} f_S(r,R_S,a_S) \\ &+ \{V_{so} + iW_{so}\}\left[\frac{\hbar}{m_\pi c}\right]^2 \frac{1}{r} f_S(r,R_{so},a_{so})(\ell\sigma) \end{aligned} \tag{1}$$

where the subscripts v, s and so indicate the volume, surface and spin-orbit terms, respectively. The $f_v(r,R_i,a_i)$ and $f_s(r,R_i,a_i)$ are the volume and surface form factors, respectively. The conventional f_v and f_s are WS and derivative WS forms:

$$f_V(r,R_i,a_i) = \frac{1}{1+\exp\left(\frac{r-R_i}{a_i}\right)} \tag{2}$$

$$f_S(r,R_i,a_i) = \frac{d}{dr} f_V(r,R_i,a_i) \tag{3}$$

where $R_i = r_i A^{1/3}$.

The real central and the imaginary surface terms have isovector terms, which depend on the asymmetry parameter $\varepsilon = (N-Z)/A$, that are denoted by V_{v1}, W_{s1} and V_{so1}. For protons (z=1) one includes the normal Coulomb scattering term $V_C(r)$ explicitly in eqn. (1). To have a unified model for neutrons and protons, one adds, respectively, the real-volume and the surface-imaginary "Coulomb shift terms" ΔV_C and ΔW_C, which account for the slowing down of the proton as it approaches the nuclear surface. All these terms lead to the final expressions for the terms in eqn. (1):

$$\begin{aligned} V_V &= V_{V0} + V_V(E) \pm \varepsilon V_{V1} - \Delta V_C \\ W_S &= W_{S0} + W_S(E) \pm \varepsilon W_{S1} - \Delta W_C \\ V_{so} &= V_{so0} + V_{so}(E) \pm \varepsilon V_{so1} \end{aligned} \tag{4}$$

In the isovector terms in eqns. (4), the (+) sign applies to proton scattering and the (-) to neutron scattering. With these definitions and sign conventions at hand, we now list the WG parameters in Table 1. Although this model was designed for 10 to 40 MeV, it might be a good guide of $\sigma(\theta)$ and $A_y(\theta)$ up to 80 MeV, since it is able to give good predictions to the 80 MeV proton data of [10]. Furthermore, even though we know that W_s must drop off somewhere around E_n = 5 MeV and decrease to about W_s = 2 MeV at E_n = 0, it has been shown [21] that the WG model is reasonably successful at predicting cross sections below E_n = 10 MeV if one merely assumes that the value that the WG potential gives at 10 MeV is valid everywhere below 10 MeV.

Table I. Optical model parameters for the Walter-Guss (WG) potential.
Potential depths are in units of MeV and lengths are in fm.

$V_{v0} + V_v(E) = 52.56 - 0.310E$		for $E \le 40$	
$V_{v0} + V_v(E) = 52.56 - 0.310\{40[1+ \ln(E/40)]\}$		for $E \ge 40$	
$V_{v1} = 16.50 - 0.081E$		for $E \le 40$	
$V_{v1} = 16.50 - 0.081\{40[1 + \ln(E/40)]\}$		for $E \ge 40$	
$W_{s0} + W_s(E) = 10.85 - 0.157E$		for $E \ge 10$	
$W_{s1} = 14.94$		Above E where $W_{s0} + W_s(E) \pm \varepsilon W_{s1} + \Delta W_{sC} < 0$, set $W_s = 0$	
$W_v = - 0.963 + 0.153E$		for $6.29 \le E \le 39.4$	
$W_v = - 0.963 + 0.153E[1 - 0.33 \ln(E/39.4)]$		for $E \ge 39.4$	
$V_{so0} + V_{so}(E) = 5.767 - 0.015E$		$V_{so1} = - 2.0\varepsilon$	
$W_{so0} + W_{so}(E) = 0.791 - 0.018E$			
$r_v = 1.219$	$a_v = 0.688$	$r_{ws} = 1.282$	$a_{ws} = 0.512$
$r_{wv} = 1.38 + 3.76/A$	$a_{wv} = 0.557 - 0.462(A^{-1/2})$		
$r_{vso} = 1.103$	$a_{vso} = 0.560$	$r_{wso} = 1.364$	$a_{wso} = 0.632$
For neutrons:	$\Delta V_{vC} = \Delta V_{vC} = \Delta W_{sC} = 0$		
For protrons:	$\Delta V_{vC} = 0.4\ ZA^{-1/3}$ for $E \le 40$	$\Delta V_{vC} = 0.4\ ZA^{-1/3}(678/E^2)$	for $E \ge 40$
	$\Delta W_{sC} = -1.30$	$R_C = r_v A^{1/3}$	
	$V_C = (zZe^2)/r$ for $r \ge R_C$	$V_C = (zZe^2/2R_C^2)[3-(r^2/R_C^2)]$	for $r \le R_C$

Table 2. Spin-orbit optical-model parameters for nucleon-nucleus elastic scattering

Ref.	Year	Mass (amu)	Energy (MeV)	V_{so} (MeV)	r_{so} (fm)	a_{so} (fm)	W_{so} (MeV)
BG[6]	‘69	45-209	$7 \le E_p \le 40$	6.2	1.01	0.75	0.0
		54-208	$1 \le E_n \le 24$	“	“	“	“
WG[11]	‘85	54-208	$10 \le E_n \le 40$	5.767-0.015E $\pm(-2.0\varepsilon)$	1.103	0.512	0.791-0.018E[a]
Var[13]	‘91	40-209	$16 \le E_p \le 65$	5.9	$1.34-1.2A^{-1/3}$	0.63	0.0
			$10 \le E_n \le 26$	“	“	“	“
Sch[10]	‘82	40-208	$80 \le E_p \le 180$	19(1-0.166 lnE) $\pm(-3.75\varepsilon)$	$0.920+.0305A^{1/3}$	0.6[b]	7.5(1-0.248 lnE)[c]
Per[5]	‘63	27-197	$9 \le E_p \le 22$	avg = 7.0	1.25	0.65	0.0
Men[8]	‘71	54-208	$30 \le E_p \le 60$	6.04	1.064	0.78	0.0
RKF[7]	‘79	40-208	$7 \le E_n \le 26$	[e]	[e]	[e]	[e]
WSS[16]	‘69	6-16	$10 \le E_p \le 50$	5.5	1.15-0.001E	0.57	0.0
Sak[15]	‘86	40-208	$E_p = 65$	avg = 4.7	avg = 1.05	avg = 0.6	avg = -0.32[d]
Wei[28]	‘96	208-209	$-20 \le E_n \le 80$	6.10-0.015E	1.126	0.559	0.791-0.018E[a]

[a] Geom.: $r_{wso} = 1.364$, $a_{wso} = 0.632$.
[b] Use 0.6 for $E_p \ge 140$ and $0.786-0.0012E_p$ for $E_p \le 140$.
[c] Geom.: $r_{wso} = 0.877+0.036A^{1/3}$, $a_{wso} = 0.62$.
[d] Geom.: average $r_{wso} = 1.46$, average $a_{wso} = 0.60$.
[e] Adopted BG parameters.

In Table 2 we summarize the parameters of spin-orbit potentials reported by various groups along with the mass and energy ranges covered in their analyses. Figure 3 is a graphical presentation of the strengths as a function of nucleon energy. In producing this graph, we assumed that the projectile is protons and that $\varepsilon = 0.1$, i.e., the mass range near ^{90}Y. This concern is only important for WG and Schwandt et al. who have an isovector component in the V_{so}. One sees that the values clump together, but it is also clear that by including the values above 80 MeV (Schwandt et al.), there is likely an energy dependence that extends to low energies as well.

Figure 3. Graphic presentation of the strength of V_{so}; values are taken from Table 2.

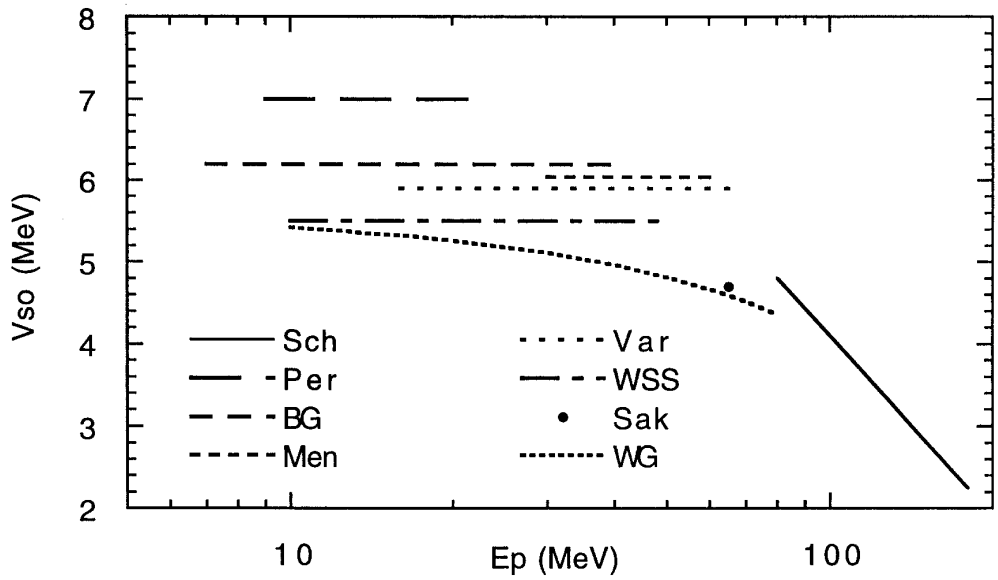

In regard to the W_{so} term, we note that the derivative in eqn. (3) will introduce an $(a_{wso})^{-1}$ factor as it does in the normal surface absorption term W_s. However, in the middle line of eqn. (1) the W_s term "anticipates" this factor by introducing a compensating a_{wso} explicitly into the formula. In addition, there is a factor of 4 inserted. (This form is conventional; when written in this way, the maximum value of $4a_{wso}\{d/dr[f(r)]\}$ is unity. The formula given in the bottom line of eqn. (1) for the absorptive spin-orbit term is also standard for this spin-orbit term; that is, the $4a_{wso}$ quantity is not part of the definition. Thus, the ratio of the quantities W_{so} to W_s is not a true measure of the relative strengths; a factor of $4a_{wso} \approx 2$ must be taken into account. Hence, a W_{so} of 800 keV relative to a W_s of 8 MeV corresponds to a ratio of approximately 1:20. All of this discussion neglects the amplification introduced by the dependence on the orbital angular momentum l through the $\boldsymbol{l}\cdot\boldsymbol{\sigma}$ factor. Likewise, the true strength of the real spin-orbit potential is not given by the quantity V_{so}, but is given by the ratio of V_{so}/a_{so}, because the derivative introduces a $1/a_{so}$. Strictly, then, the value of a_{so} should be included in comparisons of spin-orbit "interaction strengths" for different potential sets, so just comparing the strength of V_{so} as is done in Figure 3 is a bit misleading.

Since the present paper is focusing on properties of the spin-orbit term, we note the following problem. The quantity $(\hbar/m_\pi c)^2$ in eqn (1) is the square of the pion Compton wavelength and coincidentally its value is 2.000 when expressed in fm^2. It has been common to write this term in the eqn. (1) simply as the digit 2 and not mention the units fm^2. This has caused confusion when writing the value of V_{so} in MeV, as is commonly done. In a recent paper Varner et al., who used the value 2, introduced the units of MeV.fm^2 for values of V_{so}. It should be understood that when one writes 2 in eqn. (1) that the 2 carries units of fm^2 and then V_{so} is in units of MeV, the normal unit for potential strengths.

A typical set of the TUNL neutron $A_y(\theta)$ data was shown above in Figure 2. Some $A_y(\theta)$ for 65-MeV ^{208}Pb(p,p) scattering data of [15] is shown in Figure 4. Because of the relative counting rates between neutron and proton scattering and the small size of proton detectors, which allows for a large array of detectors, the proton data is more plentiful and has about an order of magnitude smaller statistical errors. The curves through the data are OM calculations by Sakaguchi et al.[15] The lower two frames shows the polarization rotation $R(\theta)$ and depolarization $D(\theta)$ parameters. The solid curves are the best fit to $\sigma(\theta)$, $A_y(\theta)$ and $R(\theta)$ including a W_{so} term. The dotted and dashed curves, respectively, are a fits to only $\sigma(\theta)$ and $A_y(\theta)$ with and without inclusion of a W_{so} term. At this energy W_{so} is found to be small, and neither $\sigma(\theta)$ nor $A_y(\theta)$ are sensitive to its inclusion except at extreme back angles. The fit to $R(\theta)$ and $D(\theta)$ is clearly improved when W_{so} is included.

The impact of V_{so} and W_{so} from 80 to 180 MeV is dramatic. The V_v is heading toward a zero crossing at slightly higher energies, and these spin-orbit terms are becoming more influential. For proton scattering, Schwandt et al. [10] observed that the oscillating $A_y(\theta)$ grows increasingly more positive in value as θ increases. The graphs of $A_y(\theta)$ in WG [11] display quite nicely that this effect holds over the entire angular range from 60° to 170° for Ni and Fe at 65 MeV and from 70° to 140° for Pb at 80 MeV; that is, in these angular ranges the $A_y(\theta)$ always ranges between about +0.8 to +1.0. Walter and Guss also show predictions for ^{54}Fe(n,n) and ^{208}Pb(n,n) for neutron energies from 30 to 70 MeV. The predictions for ^{208}Pb are reproduced in Figure 5 of the present paper. Clearly between 60° and 160° the spin-orbit term has the dominant impact on the scattering. An $A_y(\theta)$ of +1.0 means that if the incident beam is 100% polarized in the "spin-up" direction, at that angle all the particles would scatter to the left. Similarly, where $A_y(\theta) = +1.0$, if an unpolarized beam is incident, (i.e., an equal number of "spin-up" and "spin-down" neutrons in the beam) 100% of the "spin-up" will scatter to the left and 100% of the "spin-down" will scatter to the right. This must mean that the spin-orbit term has the dominant impact on the scattering, i.e., on $\sigma(\theta)$, in this angular region. Since W_{so} is nearly zero at 70-MeV, the high $A_y(\theta)$ here cannot be attributed to "spin-down" neutrons being preferentially absorbed over "spin-up" in the scattering to the left side. In our view, this "near unity $A_y(\theta)$" is one of the most interesting features in polarization phenomena.

We have noticed in our calculations that in the 10-20 MeV neutron energy range, the inclusion of a positive W_{so} value (as obtained in the WG analysis) pulls the $A_y(\theta)$ distribution to lower values over almost the entire region from 0° to 180°. One must attribute this as an *l*-dependent absorption that is less transparent to spin up neutrons on the left side than it is to spin down neutrons, and vice versa for the right side scattering. (The opposite probably occurs at higher energies where the W_{so} has changed sign.) This phenomena could not be produced by varying any other OM parameter or combination of parameters. The chi-squared values of the fit to the neutron $A_y(\theta)$ data was considerably reduced by introducing a positive value W_{so} in our OM fits to many of the data sets. An example of the sensitivity and the improvement in the fit with the WG W_{so} term is shown in Figure 2 for ^{89}Y(n,n). The data and calculations are from Honoré et al. [22]. We note that this paper also contains good pedagogical illustrations of the sensitivity of OM calculations for $\sigma(\theta)$ and $A_y(\theta)$ to variations of the strength of $V_{so}(E)$ and variations in the values for $r_{vso}(E)$ and $a_{vso}(E)$.

Figure 4. Example of proton scattering data at 65 MeV for σ(θ), $A_y(\theta)$, the rotation parameter R(θ) and the depolarization parameter D(θ). The data are for ^{208}Pb(p,p). The curves are OM calculations: (solid) best fits for σ, A_y, and R with W_{so}; (dashed) best fit for σ and A_y only without W_{so}; (dotted) best fit for σ and A_y with W_{so}. This plot is reproduced from [15].

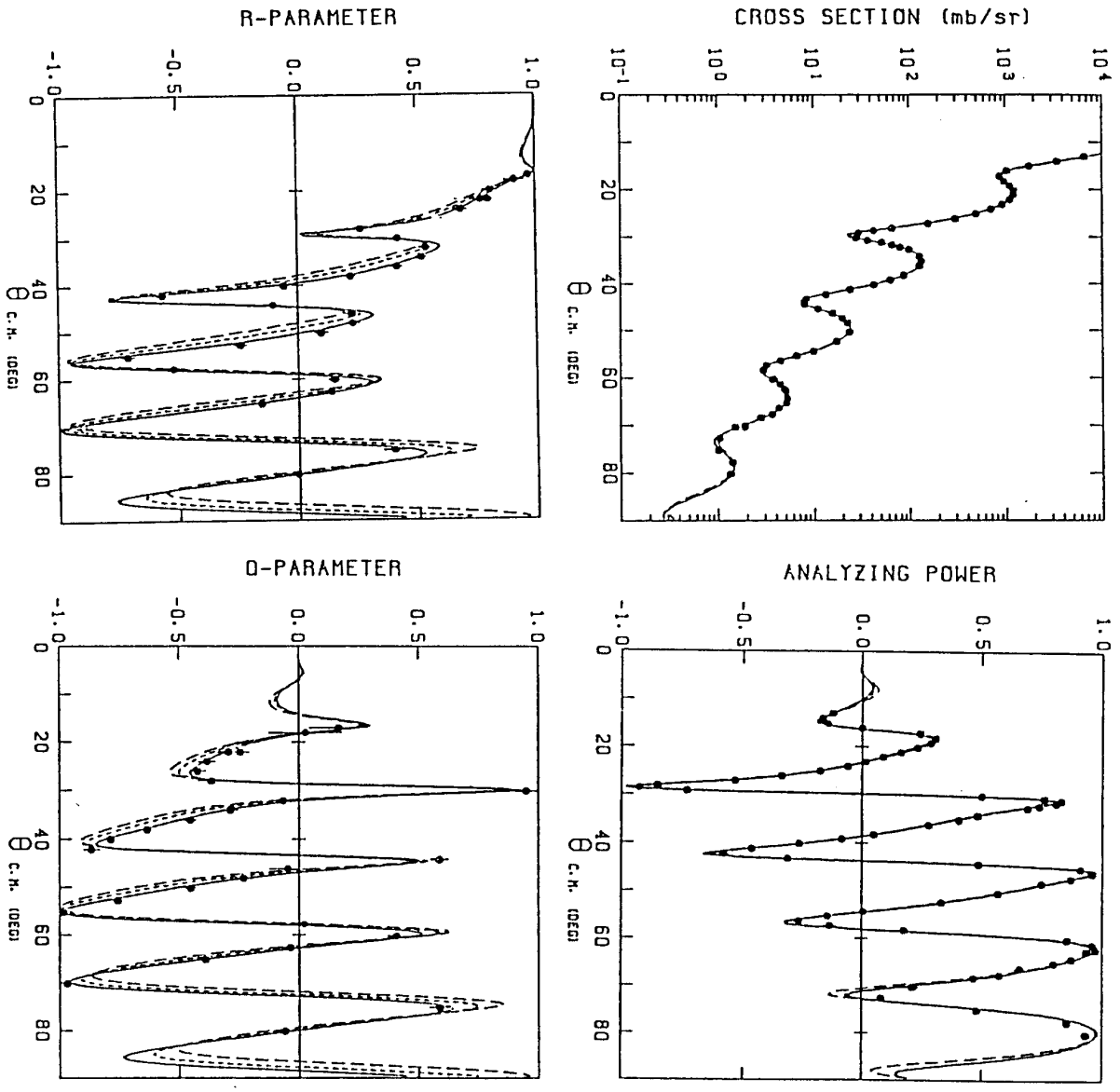

Figure 5. Calculations for ^{208}Pb(n,n) at 30 MeV, 50 MeV and 70 MeV showing the growth of the large, positive values of $A_y(\theta)$ at back angles with increasing neutron energy [11]

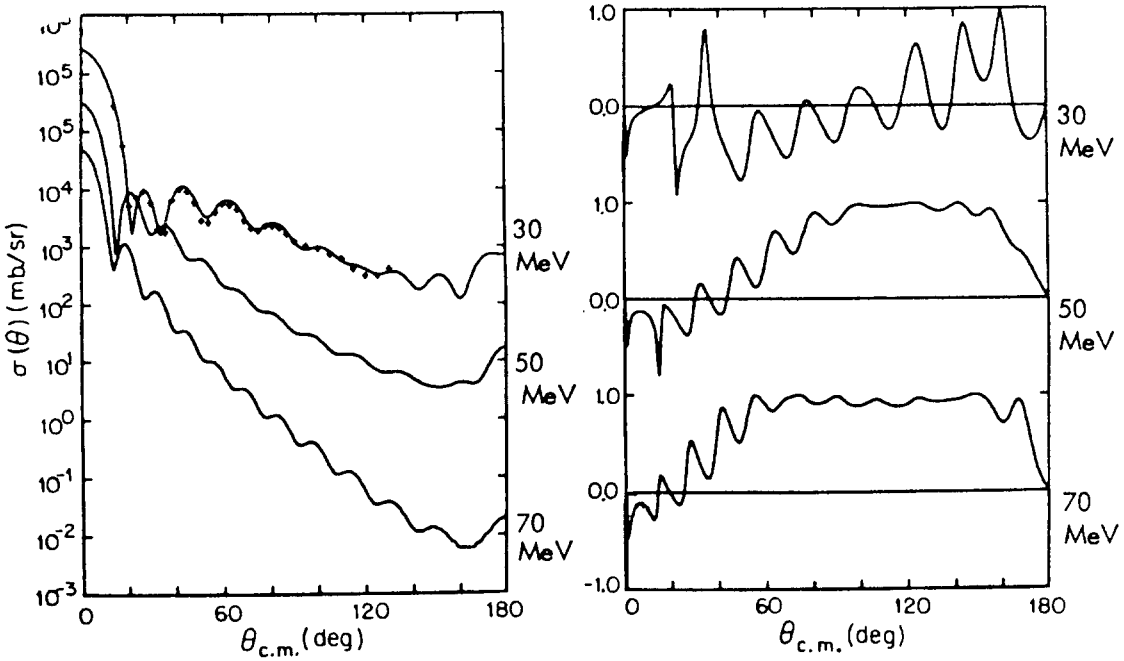

It should be remarked here that all of the OMs discussed to this point have used the non-relativistic Schrödinger equation to solve the scattering problem. Schwandt et al. [10] did use relativistic kinematics and a relativistic modification to the real potential strength. We will ignore the relativistic Dirac OM for nucleon-nucleus scattering except to comment that the model predicts a negative value [23] for W_{so} for energies above 40 MeV. An interesting review of the status of non-relativistic and relativistic models, along with the comparisons of data and predictions from 200 to 800 MeV by Ray et al. appeared in 1992.[23]

There needs to be one last comment on global models at low energies. In a global model it now seems that it makes good sense to write the E-dependent quantities in terms of the projectile kinetic energy (E) minus the Fermi energy (E_F) instead of merely E, as has been done up to this date. Mahaux [24] started to move in this direction but dropped the project. Wang and Rapaport [25] made some observations in terms of ($E - E_F$) in their study of the magnitude of the isovector term for neighboring isotopes. It seems to us that improved fits to the data could be achieved if the E-dependences were determined as functions of ($E - E_F$); we may attempt this in the near future.

V. TUNL OM analyses 2: Dispersive OM analyses

Since about 1987 there has been an increasing interest in the dispersive optical model (DOM) as a method for eliminating some of the problems with the energy dependence of the radius and strength of the real central potential at low energies. Mahaux and co-workers [26] have made many contributions to the development of this approach. They emphasized that the DOM allows one to connect the scattering regime (positive energies) to the shell model regime (negative energies). This approach has been shown to give good predictions to single-particle bound-state energies and to the scattering data without introducing any abnormal explicit E-dependences in the OM parameters. Many DOM papers have now been published for neutron-nucleus cases and a few for proton-nucleus cases.

At TUNL we have investigated about ten neutron scattering systems between $27 \leq A \leq 209$ over the energy range from about –20 to +80 MeV. In these analyses the TUNL $\sigma(\theta)$ and $A_y(\theta)$ data make up about half of the database. In addition, the relatively recent high-accuracy total cross-section σ_T data of Finlay et al. [27] has played a key role in determining the E-dependence of all the potential strengths, but in particular the volume- and surface-absorption strengths. At TUNL we use a modified spherical OM search code to scan parameter space and to minimize chi-squared in the fit to the scattering and σ_T data. Excellent agreement with the data has been achieved for nearly all the nuclei studied. An example of one of the more thorough treatments is the recent report of an isospin-consistent DOM for ^{208}Pb(n,n) and ^{209}Bi(n,n) by Weisel et al. [28] This model incorporated the innovations suggested by Mahaux and Sartor [26] i) of an absorptive potential (in the dispersion integral) that is asymmetric about EF and ii) of inserting a region centered on E = EF in which the absorptive potentials are set to zero.

The dispersion relation connects the imaginary potential to the real potential [ref JHM] through the integral:

$$\Delta V(E,r) = \frac{P}{\pi}\int_{-\infty}^{+\infty} \frac{W(E',r)}{E'-E}\,dE'$$

where P stands for the principal value. Here W represents the sum of the volume and surface terms of the imaginary potential. Note that the integral extends from –∞ to +∞ Therefore, a good knowledge of the E-dependence of W(E',r) is required before one can use the DR approach; this problem plus the speed of older computers made DR calculations difficult before about 1980.

Through the integration, one generates volume and surface contributions ΔV_v and ΔV_s, respectively, to the real central potential. The radial shapes of these contributions, which are called dispersion corrections, are identical to those of the original W_v and W_s. Therefore, through the dispersion relation (DR) for the surface imaginary term $W_s(r,E)$, the real part of the DOM potential contains a surface as well as the conventional volume component. One separates the total real potential V(r,E) into a Hartree-Fock part V_{HF} and the two dispersive contributions: $V(r,E) = V_{HF}(r,E) + \Delta V_v(r,E) + \Delta V_s(r,E)$. It is the energy dependence of both DR terms that gives V(r,E) a complicated behavior at low energies; the size and sign (which changes near 15 MeV) of ΔV_s causes the effective radius of the real central potential to vary with energy. This detail had been observed in non-DR optical model searches on data. So the DR corrections, which have a solid physical base, explain many of the previous problems associated with attempts to describe scattering data below about 15 MeV with standard OMs. Space limitations prohibit us from reproducing here the potentials that Weisel et al. found to give good descriptions to the data. (See Figures 20 to 22 in [28].) The DR corrections are reproduced here in Figure 6. Samples of the quality of agreement between the calculations and the data are shown in Figures 7 to 9 for $\sigma(\theta)$, $A_y(\theta)$ and σ_T, respectively. The same WS shapes given in eqns. (2) and (3) above were used for the base potentials and for the DR contributions.

The dispersion correction terms are calculated for only the real central potential term. No such corrections have been added yet either to the imaginary terms or to the spin-orbit terms. Therefore, it is reasonable to consider the spin-orbit parameters of DOMs in comparison to those obtained in non-DR OMs. The values of Weisel et al. have been included in Table 2; in their search they used the WG values as starting parameters for $V_{so}(E)$ and $W_{so}(E)$ and never found a need to modify the energy dependences.

In summary, the DOM is capable of describing the scattering data in a natural way that leads to simple energy dependences of the base potential terms and explains the changing radial dependence as the energy changes. Furthermore, the DOM gives a natural extension to negative energies and allows one to calculate properties of single-particle bound states. This was first done for ^{208}Pb in [29] and most recently in Weisel et al. The latter paper exhibits the sensitivity and complicated dependence of the location of the valence single-particle binding energies on the V_{so}, r_{so} and a_{so}.

Figure 6. Surface and volume dispersion-relation contributions to V(r,E). See reference [28] regarding the four sets of calculations. The "full-constr" is an isospin consistent model for Pb and Bi.

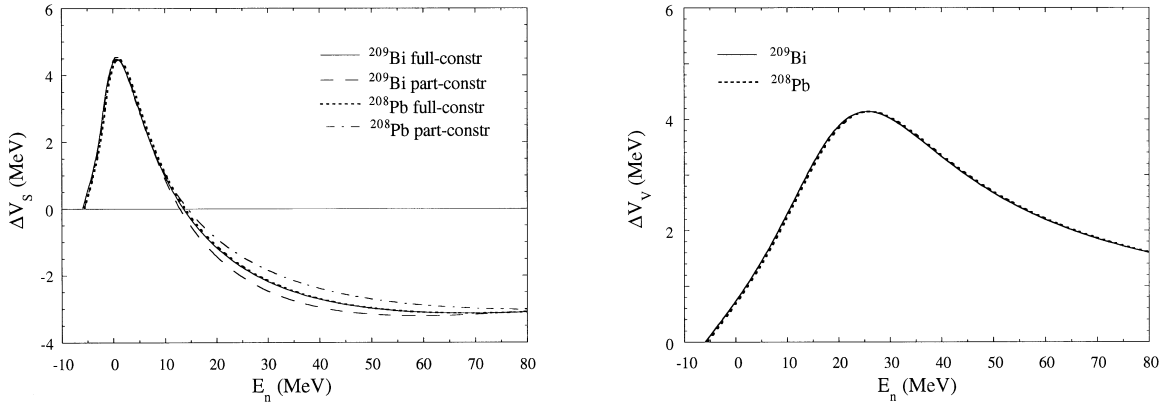

Figure 7. The DOM calculations for σ(θ) compared to data for ^{208}Pb(n,n) from 8 to 14 MeV [28]

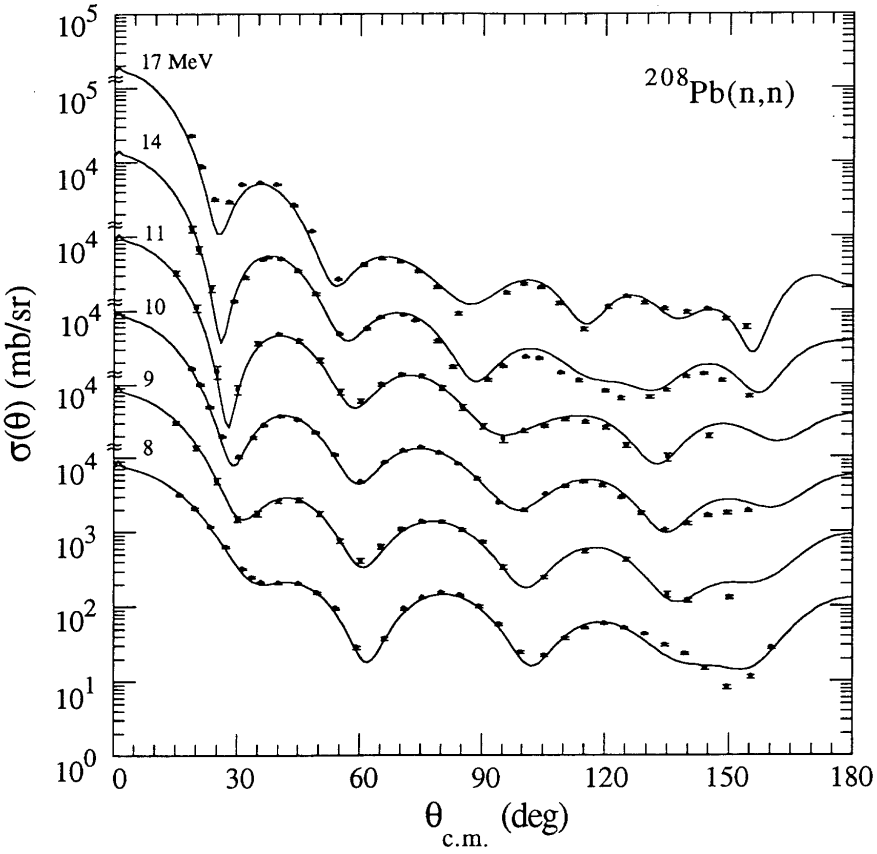

Figure 8. The DOM $A_y(\theta)$ calculations compared to data for ^{208}Pb(n,n) from 8 to 14 MeV. The barely visible dotted curves that lie close to the data are ones that include W_{so}.[28]

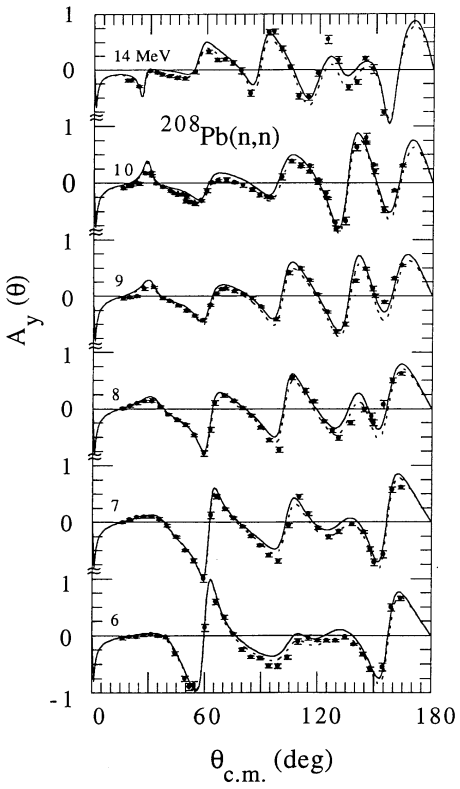

Figure 9. The DOM calculations for σ_T compared to data for ^{208}Pb and ^{209}Bi from 2 to 80 MeV. Note the zero offset on the vertical scale. The size of a 1.5% discrepancy between data and calculation is indicated.[28]

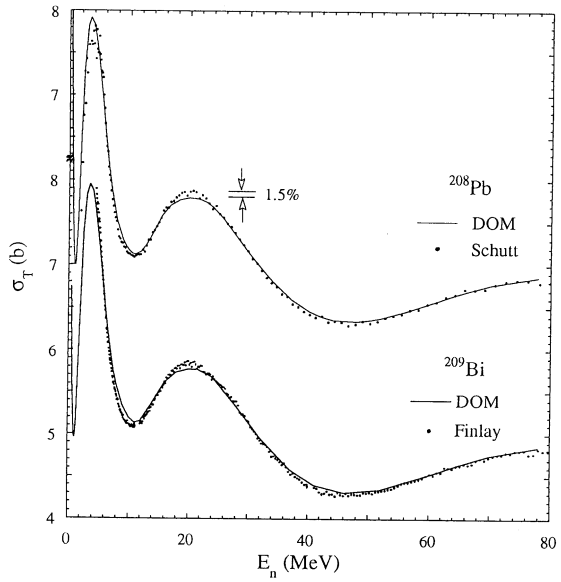

VI. TUNL OM analyses 3: Microscopic OM analyses

In collaboration with L. Hansen and F. Dietrich of LLNL we have been investigating the normalization factors λ for the three potential strengths (V, W and V_{so}) for neutron-nucleus scattering for $8 \le E \le 17$ MeV, typically, and for $6 \le A \le 208$ wherever substantial polarization data exist and for a few cases of proton-nucleus scattering. The major objective here is to concentrate on the λ_{so} and the TUNL neutron $A_y(\theta)$ data, since most of the previous neutron microscopic analyses concentrated on $\sigma(\theta)$ data. We were also curious about how well one of the more common interactions, that of Jeukenne, Lejeune and Mahaux (JLM) [30] described our $\sigma(\theta)$ and $A_y(\theta)$ data for (n,n) and (p,p) scattering for 1p-shell nuclei. This model, which has no spin-orbit term, is based on the Reid hard-core nucleon-nucleon interaction. Our JLM calculations use the real and energy independent M3Y spin-orbit interaction with Elliott oscillator G-matrix elements as given by Bertsch et al. [31] We also compared the data to calculations using the interaction of Yamaguchi, Nagata and Matsuda (YNM) [32] who based their model on the Hamada-Johnson interaction, which includes a spin-orbit term. Some of the previous analyses by Hansen and Dietrich, which can serve as an introduction to these microscopic calculations, are given in [33]. These publications indicated that good quality fits to $\sigma(\theta)$ can be achieved with both JLM and YNM interactions, provided the strengths are scaled by smoothly varying energy-dependent renormalization parameters $\lambda_V(E)$ and $\lambda_W(E)$ for the real central and the imaginary potentials, respectively.

An example of the calculations for ^{89}Y(n,n) at 10 MeV are shown in Figure 10. This kind of agreement is typical for medium weight nuclei. Our findings in this mass range are that the JLM interaction predicts details in $\sigma(\theta)$ better than YNM at 8 MeV, but the opposite is true at 17 MeV. There is a slight tendency for the YNM interaction to give better predictions to $A_y(\theta)$ than the JLM with the M3Y spin-orbit interaction.

For the lighter nuclei these microscopic calculations are not as agreeable. For example, for ^{11}B we are successful in describing the $\sigma(\theta)$ for both (n,n) and (p,p), especially at the lower end of the energy range where the second diffraction minimum has not fully evolved yet. We use the same normalization constants λ for both projectiles. The descriptions of $A_y(\theta)$ data for ^{11}B are not as successful as for $\sigma(\theta)$, however. Some results for neutron $\sigma(\theta)$ and $A_y(\theta)$ for ^{10}B are shown in Figure 11. For all the light nuclei general features of $A_y(\theta)$ data are predicted, but the overall quality of agreement is somewhat disappointing. For instance, for ^{9}Be, which is the worst agreement, the entire calculated $A_y(\theta)$ distribution lies about 0.1 to 0.2 units above the data at all energies (9 to 17 MeV). For ^{6}Li the same is true for backward angles at the higher energies; forward angle data are well fit above 10 MeV. Perhaps for the backward angles for scattering from these light nuclei, exchange effects are influencing the distributions.

Now for some general findings about the $A_y(\theta)$ calculations. Interestingly, the JLM and YNM predictions for $A_y(\theta)$ closely resemble one another. Additionally, both interactions typically do a better job of describing the $A_y(\theta)$ for (p,p) than for (n,n). We also note that the $A_y(\theta)$ do not "scale" as the λ_{so} is changed from, for instance, 0.9 to 1.7; the calculated results act as if a damping or saturation process is occurring.

On the average, the optimum normalization λ_{so} was found to be in the range of 1.3 to 1.5 for both models for all nuclei heavier than A = 10. The agreement with the ^{6}Li and ^{9}Be $A_y(\theta)$ data was improved if λ_{so} took on values greater than 2.0. This may be more an indication of a problem with the spin-orbit radial dependence that the code is generating for these light nuclei rather than a problem with the normalization factor.

For medium- and heavy-weight nuclei, the $\lambda_V(E)$ was only slightly energy dependent with a value of 0.98 ± 0.04 for JLM and about 0.95 ± 0.05 for YNM. For these same nuclei the $\lambda_W(E)$ started at about 0.7 (0.6) at 8 MeV and leveled off around 0.95 (0.7) at 11 MeV for JLM (YNM). For $6 \le A \le 11$ the $\lambda_V(E)$ were quite A-dependent. For both models it took on values of about 1.2, 1.03, 1.03 and 1.09 for ^{6}Li, ^{9}Be, ^{10}B and ^{11}B, respectively. The $\lambda_W(E)$ for JLM (YNM) for ^{9}Be, ^{10}B and ^{11}B rose from about 0.6 (0.5) at 8 MeV neutron energy to about 1.0 (0.7) at 13 MeV and rolled off to about 0.8 (0.6) at 17 MeV. For ^{6}Li the $\lambda_W(E)$ just gently rose from 0.8 (0.7) to 1.3 (1.1) as the energy increased from 8 to 17 MeV. We plan to publish our findings in a comprehensive report in the next year.

Figure 10. Microscopic OM calculations of σ(θ) and A_y(θ) for ^{89}Y(n,n) compared to data (see text)

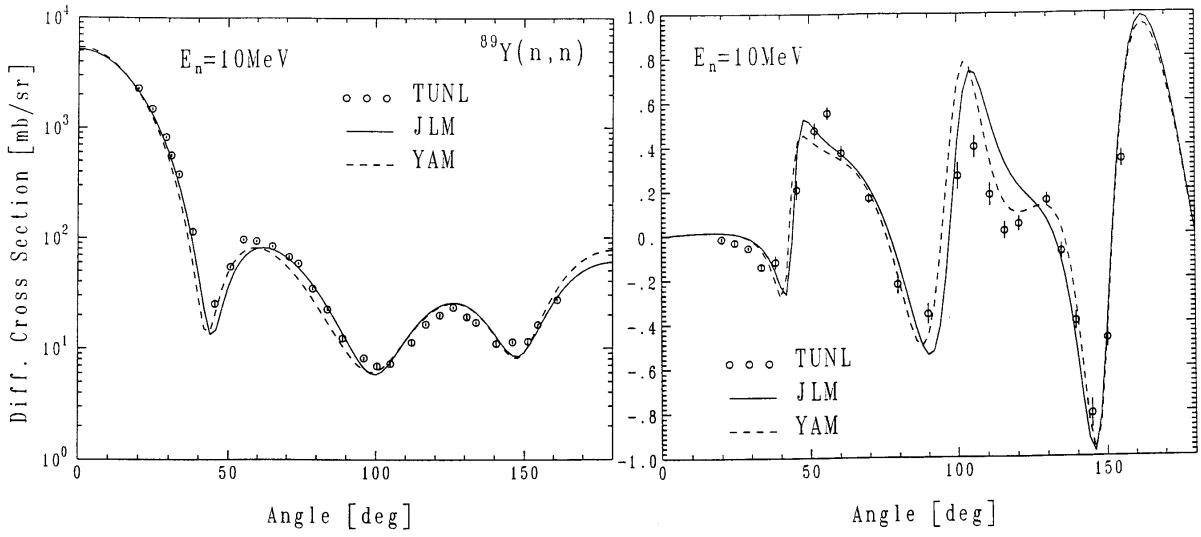

Figure 11. Microscopic OM calculations of σ(θ) and A_y(θ) for ^{10}B(n,n) compared to data (see text)

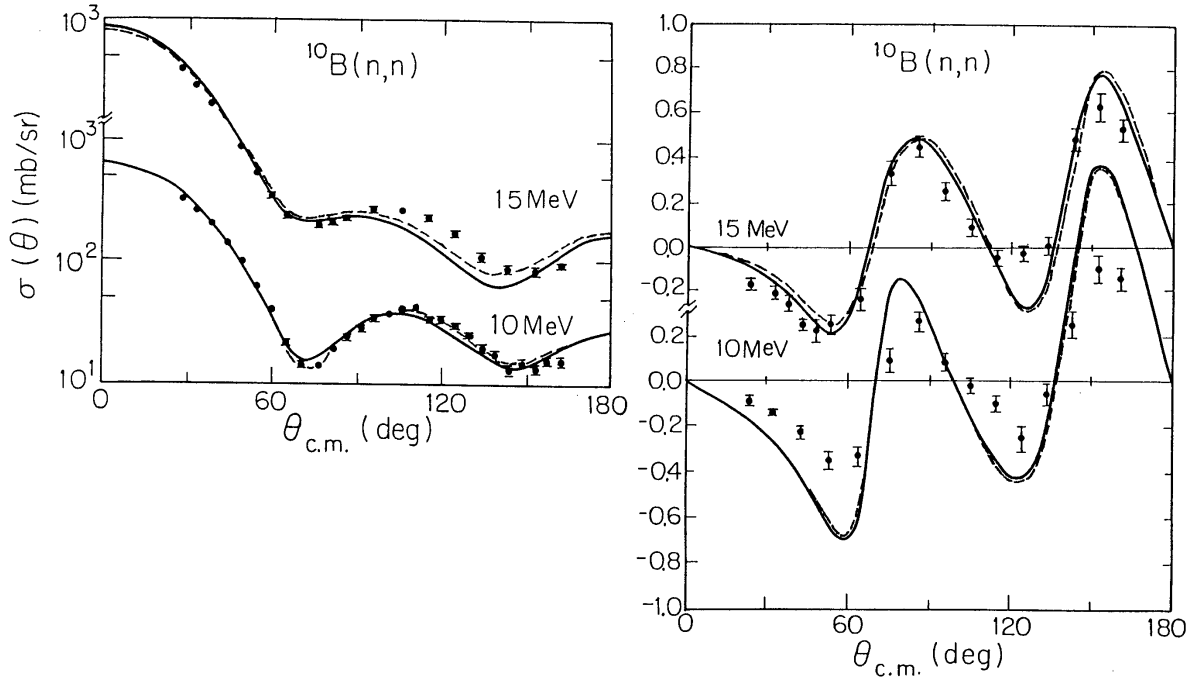

Summary statements and acknowledgements

In summary, several approaches have been used to describe cross-section and polarization data, and the models are more successful for nuclei with A > 16. The spin-orbit parameters have been fairly localized, i.e., if one accepts a Thomas-type derivative form. More investigations with Scheerbaum's microscopic prescription [34] should be made to study the significance of this approach. Below 80 MeV the $\sigma(\theta)$ and σ_T are not sensitive to modest variations in the spin-orbit parameters, except in deep minima of $\sigma(\theta)$ and at large scattering angles. Also, below 80 MeV the W_{so} has a negligible influence on cross sections; its influence even on $A_y(\theta)$ is so slight that its presence in this energy range is still controversial. (We are of the opinion that is present at the level given by the WG parameters.) Above 80 MeV the strength of the real central potential is dropping in magnitude, the spin-orbit term becomes increasingly more important factor in scattering and reactions. It will be very important to have the correct form and parametrization for $V_{so}(E,r)$ to make realistic cross-section predictions with increasing energy.

We have displayed our results for three approaches for describing the data. Important new developments [35] using the DR in coupled-channel calculations and using improved densities and interactions in microscopic calculations are just being released by Delaroche's group at Bruyères-le-Châtel. This work should contribute more fully to our understanding the features of the spin-orbit interaction.

We are grateful to the personnel in the TUNL neutron group who participated in the measurements over the years and who contributed to the analyses summarized here. We are particularly in debt to Profs. C.R. Howell and W. Tornow for the generous guidance they have provided to the students and to us. We also are thankful to the visitors from the China Institute of Atomic Energy and Tsinghua for their involvement in parts of the DOM work reported here. This project was supported in part by the U.S. Department of Energy, Office of High Energy and Nuclear Physics under Grant No. DEFG05-91-ER40619 and the U.S. National Science Foundation under Grant No. INT-9215354 (U.S.-China Cooperative Science Program).

REFERENCES

[1] P.E. Hodgson, *Nuclear Reactions and Nuclear Structure*, Clarendon Press, Oxford (1971).

[2] C.M. Perey and F.G. Perey, At. Data and Nucl. Data Tables **13**, 293 (1974).

[3] J. Rapaport, Phys. Reports **87**, 25 (1982).

[4] D. Wilmore and P.E. Hodgson, Nucl. Phys. **55**, 673 (1964).

[5] F.G. Perey, Phys. Rev. **131**, 745 (1963).

[6] F.D. Becchetti and G.W. Greenlees, Phys. Rev. **182**, 1190 (1969).

[7] J. Rapaport, V. Kulkarni and R.W. Finlay, Nucl. Phys. **A330**, 15 (1979).

[8] J.J. H. Menet, E.E. Gross, J.J. Malanify and A. Zucker, Phys. Rev. C **4**, 1114 (1971).

[9] M.P. Fricke, E.E. Gross, B.J. Morton and A. Zucker, Phys. Rev. **156**, 1207 (1967).

[10] P. Schwandt et al., Phys. Rev. C **26**, 55 (1982); see also Nadasen et al., Phys. Rev. C **23**, 1023 (1981).

[11] R.L. Walter and P.P. Guss, in *Nuclear Data for Basic and Applied Science*, edited by P.G. Young, R.E. Brown, G.F. Auchampaugh, P.W. Lisowski, and L. Stewart, (Gordon and Breach, 1986) Vol. **2**, p. 1079.

[12] R.P. DeVito, S.M. Austin, W. Sterrenburg and U.E.P Berg, Phys. Rev. Lett. **47**, 628 (1981).

[13] R.L. Varner, W.J. Thompson, T.L. McAbee, E.J. Ludwig and T.B. Clegg, Phys. Reports **201**, 57 (1991).

[14] H. Sakaguchi et al., Phys. Rev. C **26**, 944 (1982).

[15] H. Sakaguchi et al., J. Phys. Soc. Jpn. **55**, 61 (1986).

[16] B.A. Watson, P.P. Singh and R.E. Segel, Phys. Rev. **182**, 977 (1969).

[17] G. Dagge et al., Phys. Rev. ; Phys. Rev. C **39**, 1774 (1989)

[18] C. Wong, J.D. Anderson, J.W. McClure and B.D. Walker, Phys. Rev. **128**, 2339 (1962).

[19] S.T. Lam et al., Univ. of Alberta Prog. Rept. (1983).

[20] J. Dave and C. Gould, Phys. Rev. C **28**, 2212 (1983).

[21] P.G. Young, private communication.

[22] G.M. Honoré et al., Phys. Rev. C **34**, 825 (1986).

[23] S. Hama et al., Phys. Rev. C **41**, 2737 (1990); L. Ray, G.W. Hoffmann and W.R. Coker, Phys. Reports **212**, 223 (1992).

[24] C. Mahaux (private communication).

[25] Y. Wang and J. Rapaport, Nucl. Phys. **A454**, 359 (1986).

[26] C. Mahaux and R. Sartor, Advances in Nucl. Phys. **20**, 1 (1991). Also see references therein.

[27] R.W. Finlay et al., Phys. Rev. C **47**, 237, (1993).

[28] G. Weisel et al., Phys. Rev. C **54**, 2410 (1996).

[29] C.H. Johnson, D.J. Horen, and C. Mahaux, Phys. Rev. C **36**, 2252 (1987).

[30] J.P. Jeukenne, A. Lejeune and C. Mahaux, Phys. Rev. C **16**, 80 (1977).

[31] G. Bertsch et al., Nucl. Phys. **A284**, 399 (1977).

[32] N. Yamaguchi, S. Nagata, and T. Matsuda, Prog. Theor. Phys. (Japan) **40**, 459 (1983).

[33] L. Hansen et al., Phys. Rev. C **31**, 1111(1985); S. Mellema, R.W. Finlay, and F.S. Dietrich, Phys. Rev. C **28**, 2267 (1983); J.S. Petler et al., Phys. Rev. C **32**, 673 (1985); Olsson et al., Nucl. Phys. **A472**, 237 (1987).

[34] R.R. Scheerbaum, Nucl. Phys. **A257**, 77 (1976).

[35] E. Bauge and J.P. Delaroche (to be published). See also these proceedings.